

# Controlled Mixing in Microfluidic Systems Using Bacterial Chemotaxis

Min Jun Kim<sup>\*†</sup> and Kenneth S. Breuer<sup>‡</sup>

Department of Mechanical Engineering & Mechanics, Drexel University, Philadelphia, Pennsylvania 19104, and Division of Engineering, Brown University, Providence, Rhode Island 02912

**We demonstrate the use of *Escherichia coli* and their chemotactic characteristics to enhance mixing in a microchannel in a controlled and bi-directional manner. The presence of a chemoattractant in one arm of a three-junction microchannel results in an asymmetric increase in the effective diffusion coefficient of extremely high molecular weight TMR-Dextran (MW 2 000 000), which rises linearly with the concentration of attractant from a baseline value of 8–42  $\mu\text{m}^2/\text{s}$  at a concentration of 0.1 M. The response to a repellent is similar, with the opposite bias.**

The concept of a miniaturized total analysis system ( $\mu$ -TAS) is to employ micromachined features that are able to manipulate and process fluid samples with high precision and efficiency. Microfluidic devices have been used in a wide variety of applications for biological assays.<sup>1–3</sup> Key benefits of microfluidic systems include enhanced analytical performance, reduced reaction times, and reduced instrument footprints when compared to conventional analogues. The fabrication of the micro- and nanofluidic channels is relatively simple and straightforward as only conventional photolithography is required.<sup>4–8</sup> However, a serious challenge facing the development and application of microfluidics is to generate fluid motion for mixing and pumping in microfabricated systems without external actuators such as syringe pumps<sup>9</sup> or externally applied electric fields.<sup>6</sup> One potential solution is to use the nanometer-scale motors from biological systems. Recently, bacterial actuation has been reported to utilize biomolecular motors from flagellated bacteria (e.g., *Escherichia coli* or *Serratia marcescens*).<sup>10–13</sup> Flagellated bacteria contain all of the regulatory

hooks necessary to build flagella, to switch their motors on and off, to control the direction and duration of their spin, and so forth. In short, the bacterium represents a highly configurable system which can be incorporated into an engineered microfluidic system.

Peritrichously flagellated *E. coli*<sup>14</sup> swim at speeds of about 30  $\mu\text{m}/\text{s}$ , propelled by the rotation of 3–5 long (10  $\mu\text{m}$ ), thin (20 nm) helical filaments, each driven at its base by a flagellar motor.<sup>14,15</sup> The motor is powered by an electrochemical gradient that drives protons from the outside to the inside of the cell.<sup>10</sup> When all of the motors spin counterclockwise (CCW, as seen by an observer behind the cell), the filaments form a bundle that pushes the cell forward—the cell is said to run. When one or more motors spin clockwise (CW), their filaments leave the bundle and the cell body reorients (“tumbles”). When the motors spin CCW once again, their filaments rejoin the bundle, and the cell resumes its full speed, this time in a new direction. The bacteria provide a natural mechanism for achieving mixing<sup>10,14</sup>—their motion is naturally chaotic, and so by placing them in the appropriate places,<sup>11,16</sup> or even by letting them swim in the reagent soup,<sup>12</sup> mixing enhancements would be achieved.

As the bacterial cell swims, it monitors the surrounding fluid with the aid of specific chemoreceptors,<sup>14,17</sup> and the cell behavior adjusts in response to changes in the concentration of these chemostimulators as well as the levels of dissolved oxygen,<sup>18</sup> food,<sup>13</sup> temperature,<sup>19</sup> and other environmental conditions. Using this sensory hardware, cells will swim preferentially toward an increasing concentration of favorable molecules and away from potentially harmful ones.<sup>20–22</sup> This ability to control movement in response to chemical stimuli is termed chemotaxis.<sup>14,20</sup> Chemotactic bacteria contain receptors in the cell membrane that bind

\* Corresponding author. Tel: 215-895-2295. Fax: 215-895-1478. E-mail: minjun.kim@drexel.edu.

† Drexel University.

‡ Brown University.

- (1) Kopp, S. M.; de Mello, A. J.; Manz, A. *Science* **1998**, *280*, 1046–1048.
- (2) Stavis, S. M.; Edel, J. B.; Samiee, K. T.; Craighead, H. G. *Lab Chip* **2005**, *5*, 337–343.
- (3) Buchholz, B. A.; Doherty, E. A. S.; Albarghouthi, M. N.; Bogdan, F. M.; Zahn, J. M.; Barron, A. E. *Anal. Chem.* **2001**, *73*, 157–164.
- (4) Chen, Y.; Pepin, A. *Electrophoresis* **2001**, *22*, 187–207.
- (5) Reyes, D. R.; Iossifidis, D.; Auroux, P. A.; Manz, A. *Anal. Chem.* **2002**, *74*, 2623–2636.
- (6) Kim, M. J.; Beskok, A.; Kihm, K. D. *Exp. Fluids* **2002**, *33*, 170–180.
- (7) Stavis, S. M.; Edel, J. B.; Samiee, K. T.; Craighead, H. G. *Lab. Chip* **2005**, *5*, 337–343.
- (8) Eijkel, J. C. T.; van der den Berg, A. *Microfluid. Nanofluid.* **2005**, *1*, 249–267.
- (9) Liu, R. H.; Stremmer, M. A.; Sharp, K. V.; Olsen, M. G.; Santiago, J. G.; Adrian, R. J.; Aref, H.; Beebe, D. J. *Microelectromech.* **2000**, *S9*, 190–197.

- (10) Berg, H. C. *Annu. Rev. Biochem.* **2003**, *72*, 19–54.
- (11) Darnnton, N.; Turner, L.; Breuer, K.; Berg, H. *Biophys. J.* **2004**, *86*, 1863–1870.
- (12) Kim, M. J.; Breuer, K. S. *Phys. Fluids* **2004**, *16* (9), 78–81.
- (13) Kim, M. J.; Breuer, K. S. *J. Fluids Eng.*, in press.
- (14) Berg, H. C. *E. coli in motion. Biological and Medical Physics Series*; Springer-Verlag: New York, 2003.
- (15) Berg, H. C.; Anderson, R. A. *Nature* **1973**, *245*, 380–382.
- (16) Wu, X.-L.; Libchaber, A. *Phys. Rev. Lett.* **2000**, *84*, 3017–3040.
- (17) Berg, H. C.; Tedesco, P. M. *Proc. Natl. Acad. Sci. U.S.A.* **1975**, *72*, 3235–3239.
- (18) Thar, R.; Kihl, M. *Proc. Natl. Acad. Sci. U.S.A.* **2003**, *100*, 5748–5753.
- (19) Maeda, K.; Imae, Y.; Shioi, J. I.; Oosawa, F. *J. Bacteriol.* **1976**, *127*, 1039–1046.
- (20) Boyd, A.; Simon, M. *Annu. Rev. Physiol.* **1982**, *44*, 501–517.
- (21) Mao, H.; Cremer, P.; Manson, M. *Proc. Natl. Acad. Sci. U.S.A.* **2003**, *100*, 5449–5454.
- (22) Diao, J.; Young, L.; Kim, S.; Fogarty, E. A.; Heilman, S. M.; Zhou, P.; Shuler, M. L.; Wu, M.; DeLisa, M. P. *Lab Chip* **2006**, *6*, 381–388.

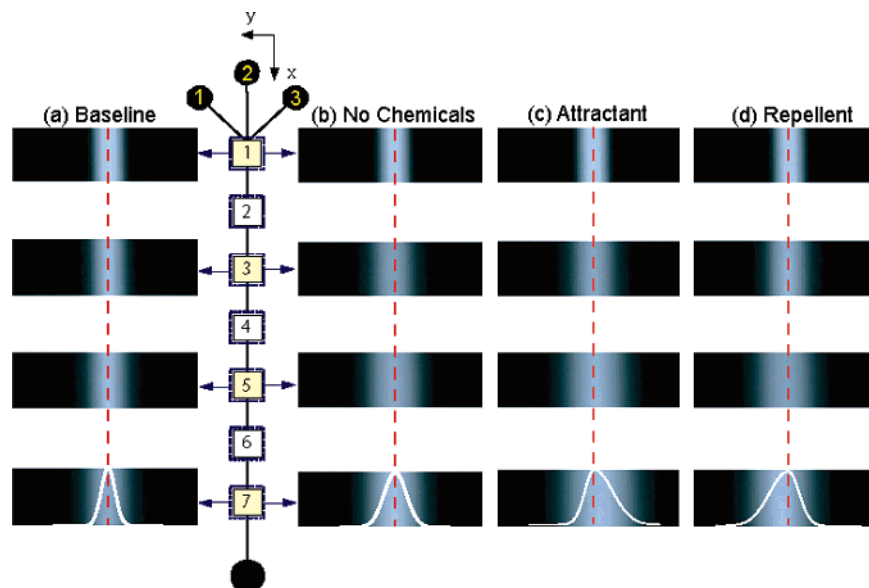


**Figure 1.** Schematic of the test geometry, illustrating the microchannel and sample diffusion profiles as they develop along the length of the channel: (a) baseline (no bacteria); (b)  $1 \times 10^9$ /mL wild-type *E. coli* in the center stream; (c) *E. coli* in the center stream and attractant in the right stream; (d) *E. coli* in the center stream and repellent in the right stream. In the main channel, we capture images at sections 1 through 7, located at  $x = 0.5, 4, 8, 12, 16, 20,$  and  $24$  mm (measured from the “ $\psi$ ”-junction).

to specific molecules and influence the balance of the run–tumble motility pattern.<sup>17</sup> When the chemical stimulus is an attractant, such as a rich nutrient source, runs that carry a cell in a favorable direction (e.g., up the gradient of a chemical attractant) are extended, biasing the bacteria’s random work in the direction of the increasing gradient. Conversely, if the stimulus is a repellent, such as a poison, a signal is sent to the flagellar motor which increases the probability of tumbling, biasing the direction of the random walk down the gradient toward more preferable conditions.

Many novel microfluidic applications powered by the motion of bacterial flagella can be envisaged. Fixing the cell bodies to a substrate (with the flagella free to rotate in the fluid) forms a *bacterial carpet* which has been observed to mix fluid,<sup>13</sup> enhance diffusion,<sup>11,13</sup> and even to collectively organize to pump fluid over a sustained period of time.<sup>23</sup> If the bacteria are not bound to the substrate, but free to swim in the fluid, augmented mixing between two streams is also achieved due to the bacterial motion.<sup>12</sup> Using the cell’s sensitivity to external stimuli, one can enhance the performance of such devices and exert control authority over a bacterial system by chemically stimulating specific behavior.<sup>13,23</sup>

One can also design a microfluidic system to measure chemotactic behavior. Mao et al.<sup>21</sup> used a controlled concentration gradient of chemoeffectors in a microfluidic device to sort bacteria according to their chemotactic sensitivity. By counting the distribution of cells at different legs of the output stream, he was able to determine the chemotactic response of a cell colony, particularly at very low chemoattractant concentrations.

In this paper, we report on a microfluidic device which uses bacteria to enhance mixing of a high-molecular-weight tracer molecule. We also demonstrate that the strength and direction of the mixing enhancement can be adjusted externally by controlling the type and concentration of a background chemoeffector.

## EXPERIMENTAL METHODS

**Cell Preparation.** Wild-type *E. coli* (HCB 33, provided by Linda Turner and Howard Berg of the Rowland Institute at Harvard University) were used in this study. *E. coli* are rod-shaped, Gram-negative bacteria about  $1 \mu\text{m}$  in diameter and  $2 \mu\text{m}$  long.<sup>14</sup> For the best motility, the  $100\text{-}\mu\text{L}$  frozen aliquot of *E. coli* was put into 10 mL of LB growth medium (10 g of tryptone, 5 g of yeast extract, 10 g of NaCl in distilled pure water) and incubated for 4.5 h at  $33 \text{ }^\circ\text{C}$ . One liter of culture medium (LB Broth) was prepared. The cultures were aerated by gently shaking the tube at about 180 rpm. The bacteria were removed from the incubator during the exponential phase of their growth for use in experiments. The *E. coli* were separated from the nutrient broth by centrifugation at  $2200g$  for 10 min, and then re-suspended in 0.5 mL of experimental buffer (0.01 M  $\text{KPO}_4$ , 0.067 M NaCl,  $10^{-4}$  M EDTA, pH 7.0) with gentle mixing. More buffer was then added to bring the total volume to 10 mL. This separation process was repeated three times to ensure that all the growth medium was removed.

**Experimental Setup.** The PDMS microfluidic device was fabricated using soft-lithographic techniques.<sup>24</sup> The three-inlet channel was in the form of a “ $\psi$ ”, with three arms, each feeding a stream of fluid into a main channel which measured  $450 \mu\text{m}$  wide,  $15 \mu\text{m}$  deep, and 28 mm long (Figure 1). The first and third arms (each 200 mm wide) carried a biological buffer solution and a low concentration (0.02% by mass) of Dextran (MW 70 000 and MW 2 000 000). The middle arm (50 mm wide) contained the same buffer and TMR (tetramethyl-rhodamine)-Dextran (MW 70 000 and MW 2 000 000). The TMR-Dextran (Molecular Probes, dye-labeled dextran conjugates) has an excitation peak at 555 nm and an emission peak at 580 nm. This is not in a spectral region that elicits a phototaxis response.<sup>25</sup> As the three streams flowed down the main channel, the stream of fluorescent molecules in

(23) Kim, M. J.; Breuer, K. S. Preprint.

(24) Whiteside, G. M.; Strook, A. D. *Phys. Today* **2001**, *54* (6), 42–46.

(25) Macnab, R.; Koshland, D. E. *J. Mol. Biol.* **2001**, *84*, 399–406.

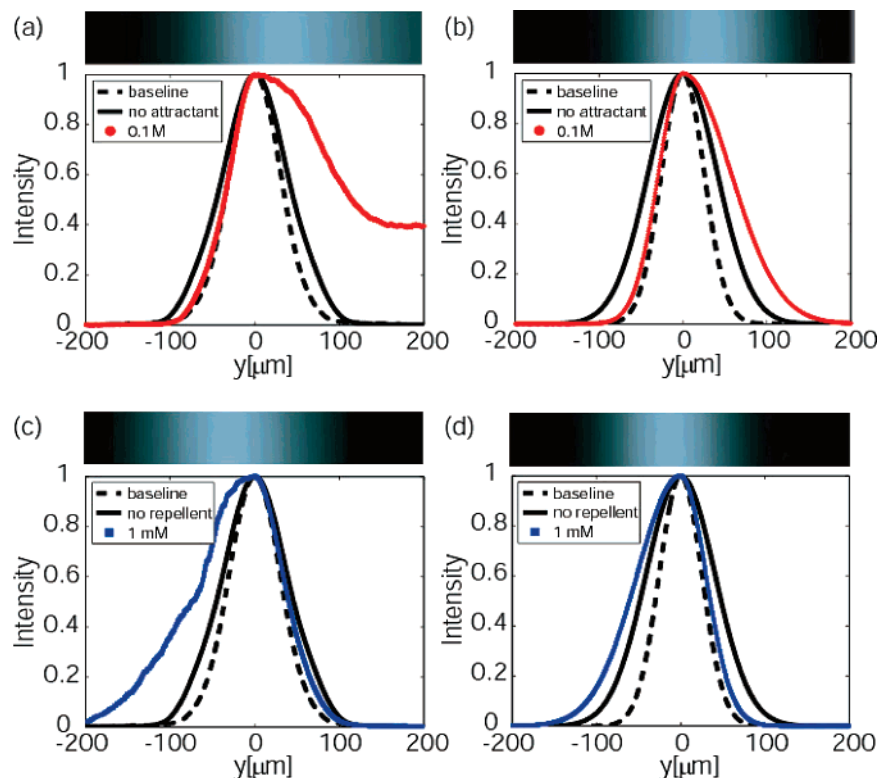


**Figure 2.** Intensity profiles at 24 mm from the “Ψ”-junction, generated from images for  $U = 0.6$  mm/s: (a) and (b) 0.1 M chemoattractant (L-aspartic acid) with a molecular weight of TMR-Dextran (MW 70 000 and MW 2 000 000), respectively, (c) and (d) 1 mM chemorepellent (nickel sulfate) with a molecular weight of TMR-Dextran (MW 70 000 and MW 2 000 000), respectively. The baseline case (dotted line) is without bacteria.

the center spread gradually due to diffusion (shown in Figure 1a). Wild-type *E. coli* were introduced at a concentration of  $1 \times 10^9$ /mL ( $OD_{600}$  of 1.2) into the fluorescent stream (the middle port). The motion of the bacteria is known to enhance the diffusion of a passive scalar such as the TMR in proportion to the concentration of bacteria<sup>12</sup> (shown in Figure 1b). However, this enhancement can be augmented and further controlled by the introduction of chemoeffectors which either attract or repel the bacteria. Chemoeffectors [L-aspartic acid (Sigma-Aldrich, St. Louis MO), which is a chemoattractant, and  $NiSO_4$  (Sigma-Aldrich), which is a chemorepellant] were introduced at low concentration into the third (right) arm of the microfluidic device. The presence of the chemoeffector biased the bacterial motion and led to an asymmetric diffusion profile (Figure 1, parts c and d).

**Data Acquisition and Processing.** A range of flow rates and concentrations of chemoeffectors (L-aspartic acid and  $Ni^{2+}$ ) introduced to the right arm of the microfluidic system were tested. The velocities of bulk fluid ( $U = 0.6, 1.0, 1.4,$  and  $2.0$  mm/s) were the volumetric flow rates divided by the cross-sectional area. Measurements were taken at seven  $x$ -locations along the main channel ( $x = 0, 4, 8, 12, 16, 20,$  and  $24$  mm, measured from the “Ψ”-junction).

The fluorescence intensity profile was imaged using a Nikon TE200 inverted epi-fluorescent microscope with a  $20\times$  objective and recorded with an IDT SharpVision 12-bit cooled CCD camera, with  $1300 \times 1080$  pixels. Ten images were recorded at each  $x$ -position along the channel and each flow rate. The intensity profile across the channel (which is proportional to the concentration of TMR) was computed by averaging the ten frames and

averaging over 1122 pixels in the streamwise direction (corresponding to  $400 \mu\text{m}$ ). Typical measured intensity profiles are shown in Figure 2, illustrating the baseline (symmetric) intensity distribution, the enhanced mixing due to the bacteria, and the asymmetric mixing induced by bacteria swimming in the presence of attractant or repellent.

The maximum value of the intensity profile and its location were determined by subpixel interpolation in which a quadratic polynomial was fit to the five pixels surrounding the maximum in the intensity peak (two to the left, two to the right). The width of the concentration distribution was estimated by calculating the standard deviation of the intensity distribution, computed by integration of the zeroth, first, and second moments of the intensity distribution using Simpson’s rule.

## RESULTS

In the absence of any chemical gradients, the intensity profile shows excellent right–left symmetry (Figure 1, parts a and b). The location of the maximum value of the intensity profile was always observed to be at the center of the microchannel. In this case, standard diffusion theory<sup>26</sup> predicts that the intensity profile across the channel is given by

$$I(y) = \frac{1}{2\sqrt{\pi D\tau}} \exp^{-y^2/2\sqrt{D\tau}} \quad (1)$$

where  $D$  is the effective diffusion coefficient, and  $\tau$  is a similarity

(26) Cussler, E. *Diffusion. Mass transfer in fluid systems*; Cambridge University Press: Cambridge, 1997.

variable,  $\tau = x/U$ . Here,  $U$  is the average velocity, and  $x$  is the distance from the mixing origin. The presence of *E. coli* in the center stream enhances the mixing, and the intensity profile spreads faster (Figure 1). Fitting the profile to the theoretical distribution (eq 1) yields an increased effective diffusion coefficient.<sup>7</sup>

In the presence of chemotactic gradients, the cells modulate their motility in response to the chemical signals in the environment and preferentially swim to one side or the other of the channel. Subsequently, the enhanced mixing due to the bacteria becomes asymmetric. The addition of an attractant (L-aspartate) to the right inlet arm “pulls” the passive tracer toward the right side of the channel (Figure 2, parts a and b), while the addition of a repellant (nickel) “pushes” it toward the left (Figure 2, parts c and d). For the same concentration of chemoeffector, small molecules (Figure 2, parts a and c) are affected much more dramatically than larger molecules (Figure 2, parts b and d). To enable quantitative analysis and to allow for determination of effective diffusion coefficients, it is necessary that the profiles not be perturbed too far from their equilibrium state, and for this reason all the subsequent experiments were performed with higher-molecular-weight TMR-Dextran (MW 2 000 000).

We can estimate the strength of the chemoeffector gradient that drives the asymmetric mixing using a similar one-dimensional diffusion theory in which the inflow condition is defined with the chemoeffector present only in the right-most stream. For such a flow, the concentration distribution,  $C(y,\tau)$ , is given by<sup>26</sup>

$$C(y,\tau) = \frac{1}{2} \left[ 1 + \operatorname{erf} \left( \frac{y}{2\sqrt{D_{\text{chemo}}\tau}} \right) \right] \quad (2)$$

where  $D_{\text{chemo}}$  is the molecular diffusion coefficient of chemoeffectors. On the basis of molecular weight, density, and Stoke-radius, the diffusion coefficients of L-aspartic acid and nickel sulfate can be estimated as 78 and 66  $\mu\text{m}^2/\text{s}$ , respectively. The predicted concentration profile is shown in Figure 3 for the case of  $\tau = 40$  s, along with the corresponding asymmetric Dextran profile that was measured for a 0.1 M chemoeffector. The location and width of the center inlet channel is shown by a shaded area at the center. We see that the chemoeffector gradient is at a maximum and is approximately constant over the central portion of the channel where the bacteria are introduced and their presence is most concentrated.

In order to numerically quantify the system response, the Dextran intensity profile was divided into a left and right side. Each half-profile was fit to a Gaussian function, and the standard deviation of this profile was computed. The width of the diffusion zone ( $\sigma$ ) is observed to increase linearly with the residence time,  $\tau = x/U$ , (Figure 4). The excellent collapse of the data using the residence time over a wide range of values of  $x$  and  $U$  confirms the validity of quasi-one-dimensional analysis. The effective diffusion coefficient,  $D$ , for characterizing random motility in bacteria can be calculated for both the right and left sides from the standard deviation ( $\sigma$ ) of the best-fit Gaussian using eq 1.

The effective diffusion coefficients were computed in this manner and are summarized in Figure 5, plotted logarithmically as functions of the concentration of L-aspartic acid and nickel sulfate. For the baseline and the pure bacteria case, there is little

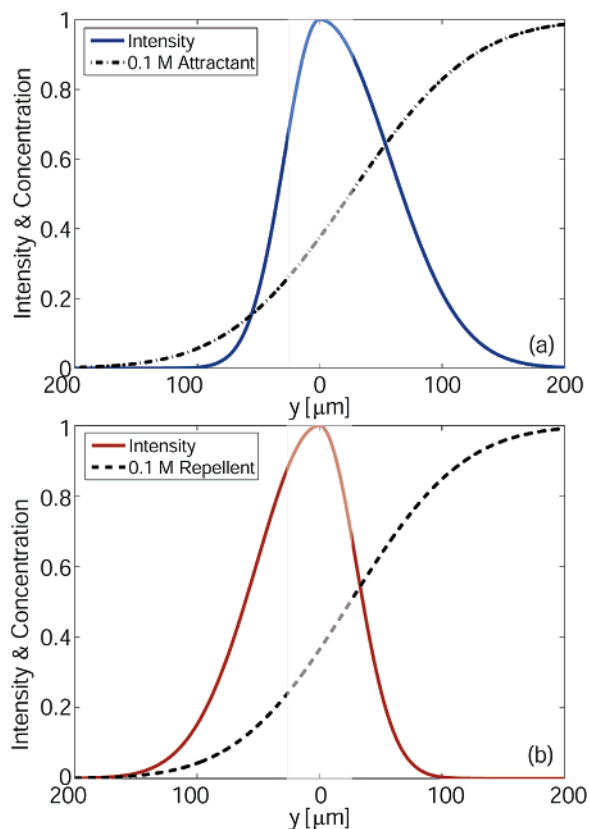


**Figure 3.** Concentration of chemoeffector and TMR-Dextran (MW 2 000 000) intensity distributions at 24 mm from the “Ψ”-junction, generated from images for  $U = 0.6$  mm/s: (a) chemoattractant (L-aspartic acid) and (b) chemorepellent (nickel sulfate). Bacteria with TMR-Dextran solution are initially infused into the band region (50  $\mu\text{m}$  wide).

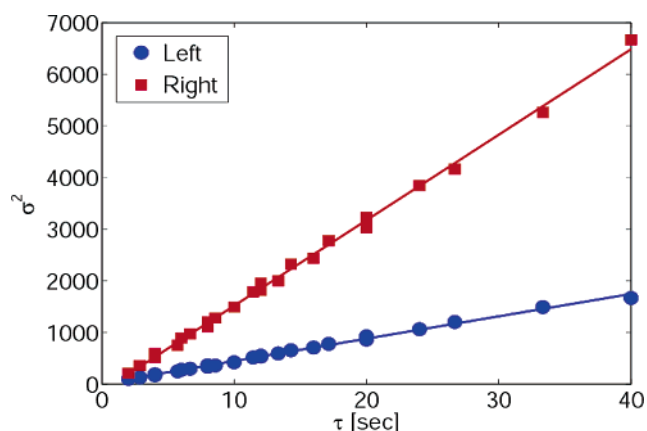


**Figure 4.** The variation of the width of the diffusion zone for the condition in which chemoattractant has been introduced to the third stream at a concentration of 10  $\mu\text{M}$  L-aspartic acid, plotted using a similarity variable.

difference between the diffusion coefficients derived from the left and right sides, and the discrepancies are within 2%. The molecular diffusion coefficient of TMR-Dextran molecules was measured as  $8.81 \pm 1.25 \mu\text{m}^2/\text{s}$ , compared with a predicted value of  $8.85 \mu\text{m}^2/\text{s}$ , based on the Stokes–Einstein equation.<sup>27</sup> The presence of pure bacteria in the middle arm, but without any chemoeffector, results

(27) Berg, H. C. *Random walks in biology*; Princeton University Press: Princeton, 1993.



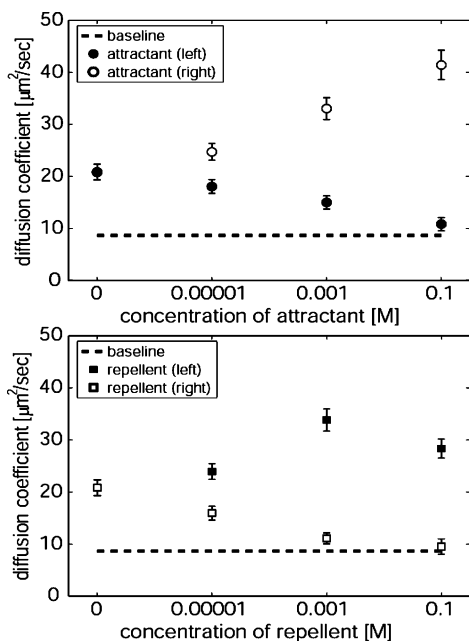


**Figure 5.** Variation of the apparent diffusion coefficient,  $D$ , as a function of the concentration of attractant (top) and repellent (bottom). The effects of adding four different concentrations of chemoeffectors (0 M, 10  $\mu\text{M}$ , 1 mM, and 0.1 M) are shown. Note that the baseline is without bacteria.

in an increase in the effective diffusion coefficient of TMR-Dextran, rising to  $20.8 \pm 1.5 \mu\text{m}^2/\text{s}$  at a concentration of  $1 \times 10^9/\text{mL}$  (approximately 0.25% by volume), consistent with previous reported results.<sup>12</sup> When L-aspartic acid is added, the diffusion on the right side increases approximately linearly, reaching an enhancement factor of 2 (four times that of the baseline with no bacteria). On the left side of the device, where there is no chemoeffector, the bacteria are nevertheless attracted toward the right side, leading to a suppression of the effective diffusion on the left side. Even 10  $\mu\text{M}$  L-aspartic acid was sufficient to skew the distribution toward the stream in which it was introduced. Placing a chemorepellent in the right stream induces the opposite effect—increasing the effective diffusion on the left side while suppressing it on the right side. The magnitude of the effect is approximately the same as that observed in the case of L-aspartate. The one exception is seen at high concentrations of nickel sulfate, in which case the “pushing” of the Dextran away from the

chemorepellent becomes weaker, presumably due to suppression of cell motility that can occur at this high concentration of the repellent.<sup>21,28</sup>

## CONCLUSIONS

We have demonstrated and quantified the use of chemoeffectors to control the spreading and mixing of a high-molecular-weight tracer molecule. Although very dramatic mixing can be achieved (Figure 2, parts a and c), we have deliberately avoided this regime in favor of more subtle enhancements, so as to be able to carefully quantify the effect. Devices based on this concept might be used to modify local solute concentrations in a fluid in a bi-directional manner and with variable amplitude simply by altering the concentrations of the aspartic acid and nickel sulfate in one or both of the control streams. By combining both the aspartic acid and nickel sulfate in the left and right streams, respectively, one should be able to achieve even more impressive control using both the pull and push effects. If the outlet path were to be subdivided, one could then use this technique to carefully control the amount of the solute (in this case, the Dextran) that is delivered into a particular outlet channel. Such devices are extremely adaptable and might be of practical use in situations where the fine control of solute concentrations is required.

A further application of this might be as a chemotactic assay, similar to that demonstrated by Mao et al.<sup>21</sup> However, in the present case, the assessment of the chemotactic response is somewhat simpler, since one does not need to sample bacterial concentrations in multiple output channels, but rather only a fluorescence intensity distribution measured at a single location downstream of the inlet.

## ACKNOWLEDGMENT

This work was supported by the Ostrach Graduate Fellowship (M.J.K.). The assistance and collaboration with Howard Berg, Linda Turner, Nicholas Darnton, Tom Powers, Greg Huber, and Munju Kim are most gratefully acknowledged.

Received for review August 8, 2006. Accepted November 9, 2006.

AC0614691

(28) Pina, K. D.; Desjardin, V.; Mandrand-Berthelot, M.-A.; Giordano, G.; Wu, L.-F. *J. Bacteriol.* **1999**, *181*, 670–674.